Int. J. Electrochem. Sci., 15 **(2020)** 6109 – 6121, doi: 10.20964/2020.07.75

International Journal of
ELECTROCHEMICAL
SCIENCE
www.electrochemsci.org

Electrochemical Evaluation of Titanium Production from Porous Ti_2O_3 in LiCl-KCl-Li_2O Eutectic Melt

Kun Zhao[1,*], *Feng Gao*[2]

[1] College of Material Science and Engineering, Yangtze Normal University, Chongqing 408100, China
[2] School of Chemistry and Chemistry Engineering, Yangtze Normal University, Chongqing 408100, China
[*]E-mail: zkngwt@126.com

Received: 4 March 2020 / *Accepted:* 5 May 2020 / *Published:* 10 June 2020

This work presents an electrochemical co-reduction of porous Ti_2O_3 in LiCl-KCl-Li_2O melt at 800 °C. Cyclic voltammetry was applied to investigate the electrochemical behavior of Li^+, Cl^-, O^{2-} and CO_3^{2-} by using glassy carbon and Pt working electrodes, respectively. The electrode reaction mechanisms and particle evolution principles in molten salt were discussed. Transient electrochemical techniques show that Ti_2O_3 is reduced to Ti metal by a two-step mechanism involving the exchanges of one and two electrons. Continually-varied current electrolysis was conducted using a porous Ti_2O_3 electrode against graphite and Pt anode in the molten LiCl-KCl-Li_2O electrolyte medium at 800 °C respectively to gain insight into the electro-reduction mechanism. The results showed the oxide component was electro-deoxidized effectively and Ti metal was produced as the final product in the cathode. Our work suggests that developing a low-cost inert anode material is essential for the production of titanium by electrolysis in the future.

Keywords: Titanium; Continually-varied current electrolysis; Porous electrode; Ti_2O_3

1. INTRODUCTION

The use of the electron as a reductant in electro-deoxidation for the preparation of titanium is known as a technique relatively simple, inexpensive, and eco-friendly [1, 2]. As the most typical representative, the FFC Cambridge process based on the direct electrochemical reduction of TiO_2 in molten $CaCl_2$ has been reported to be successful in small trials and considered to be more promising to replace the current titanium production process——The Kroll process [3, 4]. The main mechanism of the FFC process is the ionization of cathode TiO_2 in molten chlorides under the driving of the potential that is lower than the thermodynamic decomposition potential of the electrolyte but sufficient to decompose the metal oxide to the metal. The ionized oxygen passes into molten salt and reacts with

graphite anode to evolve CO or CO_2. The electro-deoxidation of TiO_2 pellets in molten $CaCl_2$ was studied by Schwandt et al [5]. The results showed that the electrochemical reduction of TiO_2 in molten $CaCl_2$ was achieved by the formation and decomposition of Ca-Ti-O compounds and titanium sub-oxides. The reduction pathway to the sequence of reactions follows as $TiO_2 \rightarrow Ti_4O_7 + CaTiO_3 \rightarrow Ti_3O_5 + CaTiO_3 \rightarrow Ti_2O_3 + CaTiO_3 \rightarrow CaTi_2O_4 + TiO \rightarrow Ti_2O \rightarrow Ti$. Ho-Sup Shin et al. investigated the electrochemical reduction of TiO_2 powder in molten LiCl [6, 7]. The reduction pathway is $TiO_2 \rightarrow LiTi_2O_4 \rightarrow LiTiO_2 \rightarrow TiO \rightarrow Ti_2O \rightarrow Ti$.

Most of the previous works are devoted to the production of Ti used TiO_2 [8–12]. However, compared with TiO_2, titanium sub-oxides possess a better electrical conductivity at a certain temperature due to the unique structure. Among these compounds, Ti_2O_3 is the lowest oxide before forming Ti-O-C via carbothermal reduction, which means it can be produced easily [13]. Besides, when Ti_2O_3 serves as the cathode above 650 °C, the electrolytic efficiency can be improved significantly through accelerating the electrochemical process [14]. In this paper, the possibility of electrolysis using a porous Ti_2O_3 electrode in LiCl-KCl-Li_2O melt as a new process of Ti production was investigated. Compared with electrolysis using TiO_2, this method shortened and simplified the reduction pathway to producing Ti.

2. MATERIALS AND METHODS

2.1 Raw materials

Anhydrous LiCl, KCl, Li_2O and Li_2CO_3 (≥99%, analytical grade) purchased from Sinopharm Chemical Reagent Company Limited were used for electrochemical tests and electrolysis process in this work. LiCl, KCl, and Li_2O/Li_2CO_3 were weighed and mixed with a fixed molar ratio. The eutectic mixture was first dried under vacuum for 48 h at 423 K to remove moisture completely. Ti_2O_3 was prepared by the carbothermal reduction of TiO_2 using activated carbon as the reducing agent at 1350 °C [15–17]. Fig.1a indicates the XRD pattern of the sintered porous Ti_2O_3 electrode in which all peaks visible correspond to Ti_2O_3. The result presents that there is no new phase yielded during the sintering process. The SEM photograph of the sintered porous Ti_2O_3 electrode shown in Fig.1b. It suggests a porous homogeneous structure. Porosity existed is favorable for the penetration of molten salts and the diffusion of ionized O^{2-} during electrolysis. The porosity of Ti_2O_3 electrode was estimated to be 60%~70% by the measurement of a mercury porosimetry (Auto Pore IV 9500, Micromeritics Instrument Corp.). The porous product obtained from the carbothermal reduction was directly used as an electrode in electrolysis experiments, the photo of that was illustrated as the inset of Fig.1b.

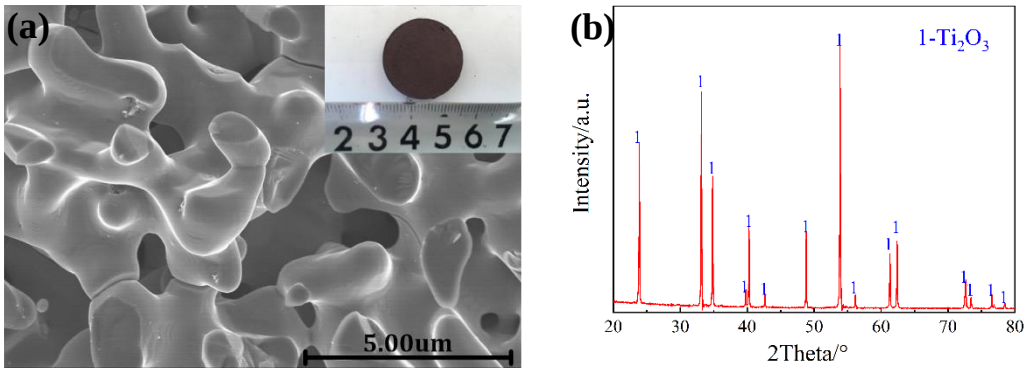

Figure 1. XRD pattern (a) and SEM image (b) of porous Ti_2O_3 electrode used for electrolysis, the insets in (b) is the photo of the porous Ti_2O_3 electrode.

2.2 Electrochemical methods

A programmable electrical resistance furnace equipped with a thermal controller was used for heating purposes. Electrochemical experiments were performed using a three-electrode system. A 20-mm-wide high-purity graphite sheet served as the counter electrode (CE). An electrode, composed of a silver wire, 1 mm in diameter, dipped into a boron nitride tube containing a silver chloride solution with a small hole giving access to the melt, was served as a Ag^+/Ag reference electrode (RE). A tungsten wire, 2 mm in diameter, was used as the working electrode (WE) for a blank experiment. Afterward, a tungsten wire working electrode with a groove full of the Ti_2O_3 porous particles (W-Ti_2O_3 electrode) was utilized to recognize the reduction mechanism. In addition, another two different types of working electrode (WE) were used in the electrochemical procedure for studying the process of anode polarization: one is a glassy carbon rod (2 mm in diameter), another is a Pt wire (1mm in diameter). Cyclic voltammetry (CV) and other transient electrochemical techniques were performed using a Princeton PARSTAT 2273 electrochemical workstation and a power amplifier (BOOSTER20A, KEPCO).

The electrolysis process was carried out using a DC regulated power supply (IT6722A, ITECH) and monitoring and acquisition of the electrical data were accomplished with the help of a data acquisition system (Agilent 34401A) with a two-electrode cell. 464.5 g of LiCl-KCl-Li_2O was introduced in a high-pure graphite crucible and then placed in the sealed stainless steel chamber. A porous Ti_2O_3 cathode connected with a tungsten wire was used as the cathode. Two kinds of electrolytic processes with a graphite electrode (60 mm×80 mm) and a Pt electrode (40 mm×50 mm) as anode were implemented separately under appropriate conditions. The mixture was kept under inert Ar flow at 5 L/min during its melting. After the temperature had been attained 800 °C, the porous Ti_2O_3 cathode was slowly lowered into the electrolyte. The selected anode was then immersed in the molten salt. The power supply was then connected to the anode and cathode connection leads. Continually-varied current electrolysis on different values was performed with the corresponding voltage and electrode potential measured. Electro-reduction was terminated and the electrodes were removed from the melt into the upper part of the reactor. Then, the reactor turned cool. The salt adhering to the samples was removed by water impregnation and the cleaned samples were dried under vacuum at room temperature.

The cathode product was characterized by X-ray diffraction with a Cu-Kα characteristic ray (XRD, X′ Pert Pro MPD, Philips) and scanning electron microscopy (SEM, S-4800, Hitachi). LECO analyses (ON736 and SC832, LECO, Laboratory Equipment Corporation) were used for oxygen analysis of the product. The lithium content in reduced samples was tested on Agilent ICP-MS 7900. The used molten salt was dissolved in distilled water. After filtering the solution, excess $BaCl_2$ solution (0.5 mol/L) was added to the filtered solution to estimate the CO_3^{2-} content in the used electrolyte medium by weighing the deposit.

3. RESULTS AND DISCUSSION

3.1 Thermodynamic considerations

Fig.2 shows the standard potentials vs. Li^+/Li of possible cathode and anode reactions during the electrochemical reduction of Ti_2O_3 in LiCl-KCl-Li_2O melt at 800 °C [18]. For the anode process, reaction 7 (carbon consumption) is more favorable in thermodynamically when a graphite anode is employed. Thus, the concentration of CO_3^{2-} in molten salt would increase as the electrolysis proceeds. As a result, the cathodic reaction graduates into the deposition of carbon (reaction 5) from the electrochemical reduction of Ti_2O_3.

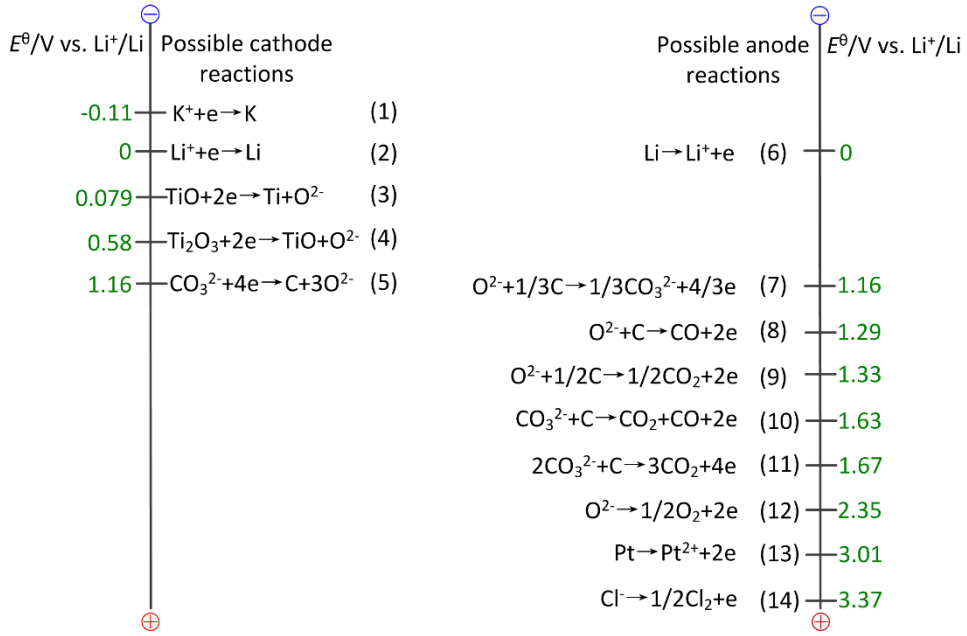

Figure 2. Standard potentials of the possible electrode reactions involved during electrolysis of Ti_2O_3 in LiCl-KCl-Li_2O melt at 800 °C using graphite and Pt electrode as the anode.

In theory, CO_3^{2-} concentration in melt will achieve a dynamic equilibrium between carbon deposition at cathode and carbon consumption at anode. However, as the cathode potential shifts negatively and the anode potential shifts positively, the equilibrium could not be maintained for three reasons: (i) more O^{2-} brought from Ti_2O_3 at cathode would enter the molten salt; (ii) metallic Li would

deposit at cathode; (iii) CO, CO_2, and even Cl_2 gas might be liberated at anode. Moreover, the complete reduction of Ti_2O_3 to metallic Ti requires the cathodic potential approaching the deposition potential of metallic Li from Fig.2. When a Pt anode is employed, it is found that O_2 evolution is more favorable thermodynamically. With the positive shift of potential, the dissolution of Pt metal occurs before Cl_2 evolution. Concurrently, the cathodic reactions are mainly contained of stepwise reduction of Ti_2O_3 and deposition of metallic Li with the negative shift of potential.

3.2 Electrochemical analysis

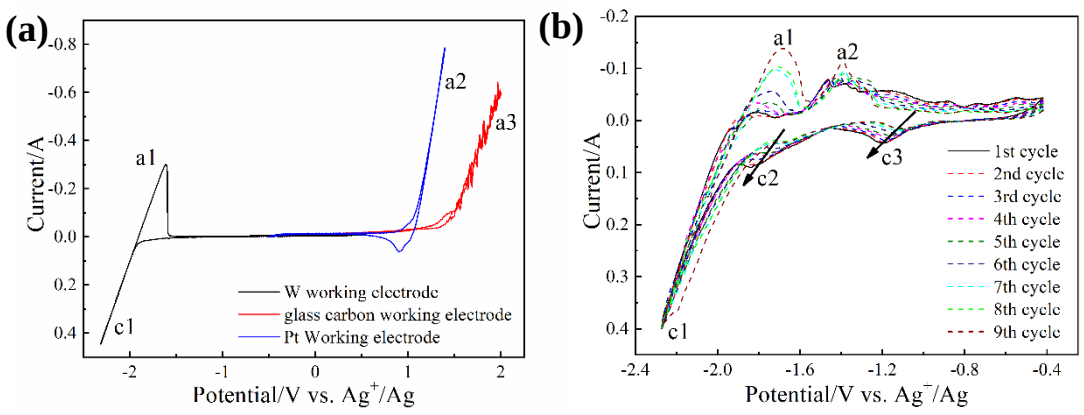

Figure 3. Cyclic voltammograms for (a) cathode and anode polarizations obtained on a different electrode (cathode polarization-W working electrode, anode polarization-glassy carbon and Pt working electrode) and (b) obtained on MCE of W-Ti_2O_3 in LiCl-KCl (46% LiCl, 54% KCl) melt at 800 °C.

Fig.3a shows the typical CV curves obtained in molten LiCl-KCl at 800 °C. For investigating the polarization process under the condition of stable electrode, cathodic and anodic polarization were carried out on W, glassy carbon, and Pt electrode respectively. From the CV curve of cathodic polarization obtained by using a W electrode, a sharp increase of cathodic current (wave c1) and the corresponding anodic current (wave a1) were observed at around –1.9 V, which were attributed to the deposition and dissolution (reaction 2 and 6, respectively) of metallic Li. Similarly, from the CV curve of anodic polarization with Pt electrode, a sharp increase of the anodic current and the corresponding cathodic current could been observed at about 1.1 V, which were brought from the dissolution and deposition of Pt. When the glassy carbon was used as the working electrode, a current was noticed to increase linearly with potential beyond 1.4 V, and it is a typical wave of the evolution of Cl_2 gas (reaction 14).

As presented in Fig.3b, a series of normalized voltammograms was recorded in the LiCl-KCl bath using the W-Ti_2O_3 electrode at 800 °C. The potential sweep ranging of the CV curves for studying the reduction of Ti_2O_3 is from –0.2 to –2.3 V (vs. Ag^+/Ag). Comparing with the CV curve of cathodic polarization obtained by using a W electrode in Fig.3a, it indicates that wave c1 observed from Fig.3b was corresponding to the deposition of Li. According to the calculated reduction potential of Ti_2O_3 and TiO in Fig.2, waves c3 and c2 could represent the reduction of the Ti_2O_3 to TiO and TiO to metallic Ti,

respectively. The electrochemical reduction of Ti_2O_3 can be summarized as Equation 15–18 by considering $LiTiO_2$ is an inevitable intermediate product during the electrochemical reduction of Ti_2O_3 in molten LiCl-KCl-Li_2O. Accordingly, wave c3 was identified to correspond to reaction 15 and wave c2 corresponded to reaction 16–18.

$$Ti_2O_3+Li^++e\rightarrow LiTiO_2+TiO \quad (15)$$

$$LiTiO_2+e\rightarrow TiO+Li^++O^{2-} \quad (16)$$

$$LiTiO_2+e\rightarrow Ti+Li^++O^{2-} \quad (17)$$

$$TiO+2e\rightarrow Ti+O^{2-} \quad (18)$$

3.3 Electrolysis of Ti_2O_3 with a graphite electrode as anode

In order to inhibit the generation of Cl_2 during the electrolysis process and elucidate the evolution principle of C, O, and CO_3^{2-}, the LiCl-KCl-Li_2O and LiCl-KCl-Li_2CO_3 melts were examined by cyclic voltammetry on a glassy carbon electrode at 800 °C. The result is shown in Fig.4. Seen from the CV curve obtained in the LiCl-KCl-Li_2O melt, two anodic waves (a2, a3) were observed. Referring to the calculated discharge potentials of O^{2-} in Fig.2, waves a2 and a3 should correspond to reactions 7 and 9. In the case of anodic polarization in molten LiCl-KCl-Li_2CO_3, three anodic waves were observed. Obviously, the wave a5 corresponds to the evolution of Cl_2. The waves a1 and a4 were corresponding to the reduction (reaction 5) and discharge (reaction 10 and 11) of CO_3^{2-}, respectively [19]. In addition, the discharge potential of CO_3^{2-} is much more positive than that of O^{2-} on glassy carbon electrode.

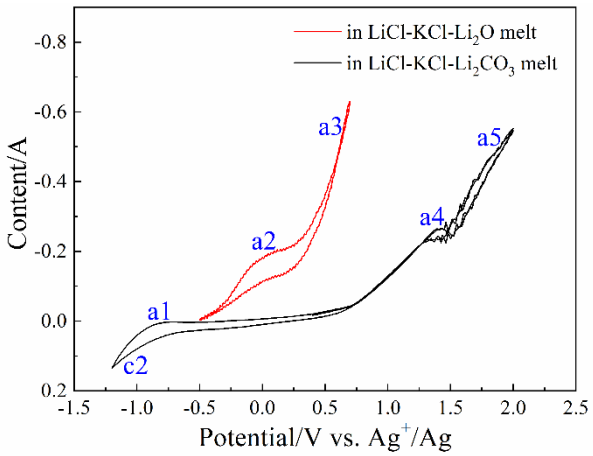

Figure 4. Cyclic voltammograms for anode polarization on a glassy carbon electrode in different melts (LiCl: KCl: Li_2O=45.6: 53.4: 1wt% and LiCl: KCl: Li_2CO_3=45.2: 52.8: 2 wt%) at 800 °C.

Continually-varied current electrolysis on different values (3 A, 4 A, 4.5 A and 5 A) with a plate electrode of porous Ti_2O_3 using as the cathode was performed in molten LiCl-KCl-Li_2O at 800 °C. The relationships between time and voltage, cathodic and anodic potential are presented in Fig.5a.

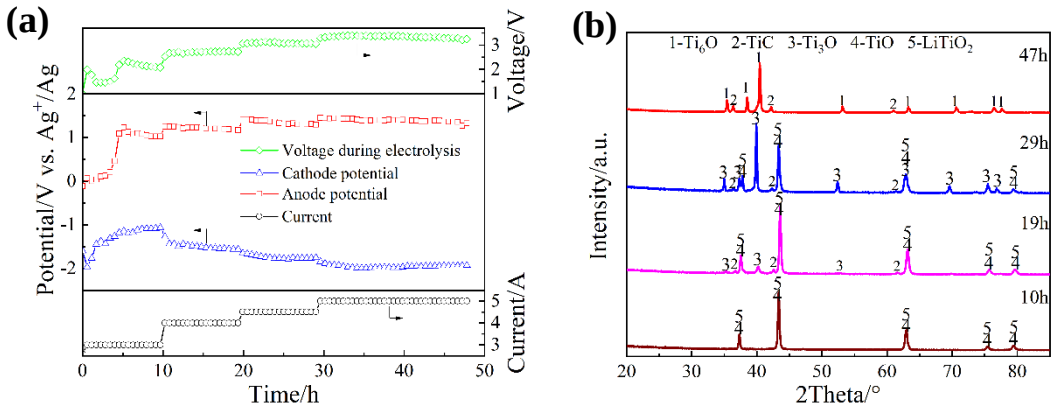

Figure 5. Electrolytic parameters versus time curves (a) for continually-varied current electrolysis on different values using a graphite anode and XRD traces (b) of the reduced samples obtained after electrolysis for different duration in LiCl-KCl-Li_2O melt at 800 °C.

It observed that the voltage follows the current step. At the first stage, the cathodic potential finally reached –1.07 V as the electrolysis continued on 3 A for 10 h, which is close to the deposition potential of carbon (reaction 5). The starting anode potential was about 0.1 V, which approach to the potential corresponding to the wave a2 in Fig.4. It shows that the starting reaction at anode could be considered as the consumption of carbon anode (reaction 7). The positive shift of both anodic and cathodic potentials at the first stage indicated that the content of active ions (O^{2-} and CO_3^{2-}) in the molten salt might have changed. It can be known from previous electrochemical analysis, the discharge potential of O^{2-} ions (reaction 7) is much more positive than that of CO_3^{2-} ions (reaction 10 and 11) on a glassy carbon electrode. Furthermore, the discharge potential of CO_3^{2-} ions (reaction 5) at the cathode is much more positive than the deposition potential of Li^+ and the electrochemical reduction potential of TiO and $LiTiO_2$. As a result, both the anodic and cathodic potentials shifted positively with O^{2-} ions decreased and CO_3^{2-} ions increased in melts at the initial stage of electrolysis. From the electrolytic current increases to 4 A, the cathodic potential became more and more negative and the anodic potential became more and more positive with the increasing of electrolytic current. When raising the electrolytic current to 5 A, the cathodic potential could achieve on –1.95 V. It proved that the deposition potential of metallic Li had been reached at 800 °C.

Fig.5b shows the XRD traces of the product obtained after continually-varied current electrolysis for different duration. It indicates that TiO and $LiTiO_2$ as intermediate products could be obtained during the continually-varied current electrolysis progress. Further increase the electrolytic current and extend the time, T_3O and TiC could be identified. The formation of Ti_3O and TiC could be attributed to the following reactions:

$$TiO+CO_3^{2-}+6e \rightarrow TiC+4O^{2-} \quad (19)$$

$$LiTiO_2+CO_3^{2-}+8e \rightarrow TiC+Li^{+}+5O^{2-} \quad (20)$$

$$3TiO+4e \rightarrow Ti_3O+2O^{2-} \quad (21)$$

$$3LiTiO_2+10e \rightarrow Ti_3O+3Li^{+}+5O^{2-} \quad (22)$$

Finally, the product of Ti with a small amount of TiC doped was obtained after continually-varied current electrolysis for 47 h. It can be inferred that a little TiC formed on the surface of samples due to CO_3^{2-} ions discharged on the surface of the cathode.

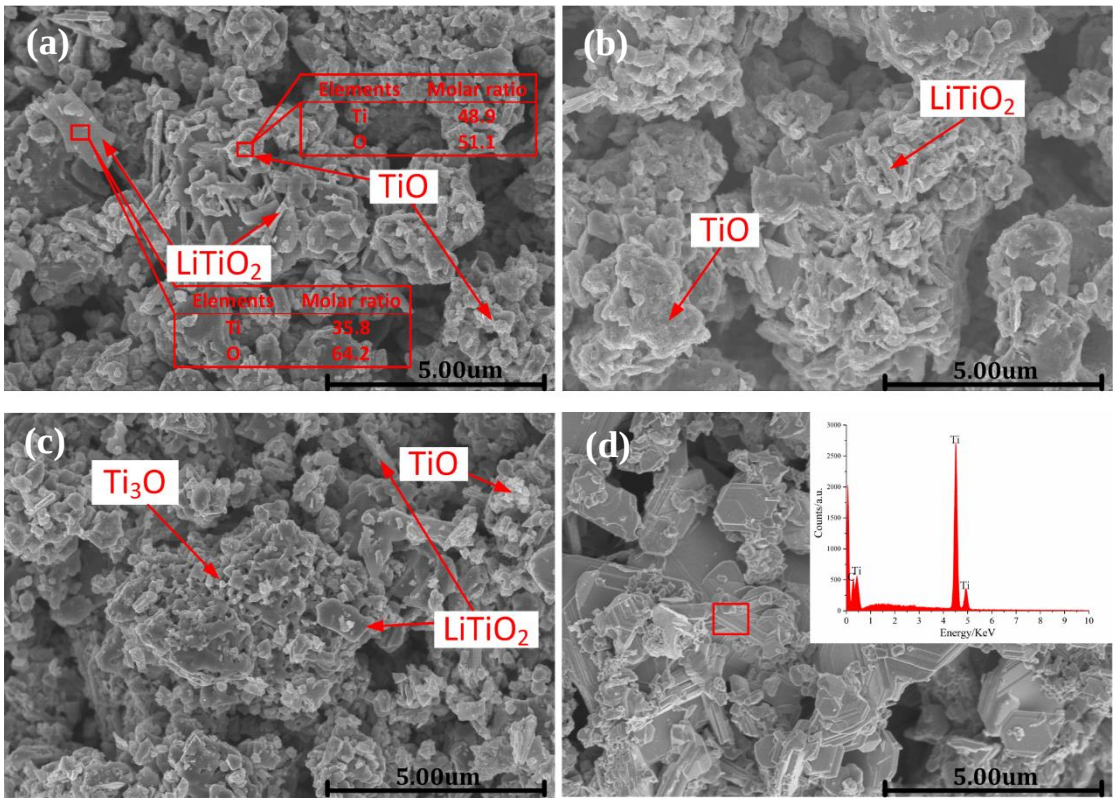

Figure 6. SEM images and EDS analysis results of the reduced samples obtained after continually-varied current electrolysis for 10 h (a), 19 h (b), 29 h (c) and 47 h (d) in LiCl-KCl-Li_2O melt at 800 °C.

The SEM images and EDS analysis results of cathodic products obtained after continually-varied current electrolysis for different duration are shown in Fig.6. The $LiTiO_2$ and TiO particles can be distinguished clearly seen from Fig.6a. After continually-varied current electrolysis on 4 A for 9 h, product morphology had no changed significantly seen from Fig.6b. A porous structure was observed from Fig.6c. It was identified as the typical structure of sintered Ti_3O according to the XRD pattern in Fig.5b. Fig.6d shows the SEM image of the reduced sample after 47 h of electrolysis. Ti particles presented scalariform.

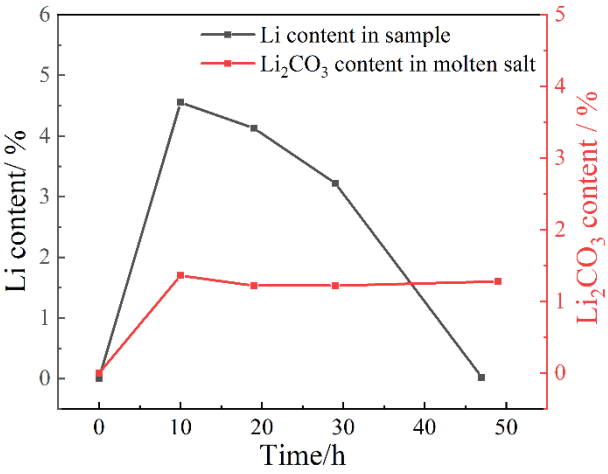

Figure 7. The Li/CO_3^{2-} contents in the cathodic product and melt concerning the different electrolysis times during continually-varied current electrolysis using a graphite electrode in LiCl-KCl-Li_2O melt at 800 °C, respectively.

From thermodynamic analysis and electrochemical tests, the electrolysis system contains a balance of carbon and oxygen. The carbon anode was oxidized and combined with O^{2-} ions to form CO_3^{2-}. When CO_3^{2-} accumulates enough, it will discharge at cathode to form C and O^{2-} ions. Obviously, the amount of the CO_3^{2-} depends on that of O^{2-} ions in molten salt. Because testing the concentration of O^{2-} ions was difficult, we mainly tested the CO_3^{2-} ion in molten salt. In order to understand the electrochemical reduction process, the Li content in cathode at different stages was also detected. The results are plotted in Fig.7. It can be seen that the Li content in cathode and the concentration of CO_3^{2-} in melt increased greatly in the first stage of constant current electrolysis with 3 A for 10 h. Therefore, the main cathodic reaction in the initial stage was the intercalation of Li^+ ions into the porous cathode, and the main anodic reaction was the consumption of carbon anode. After raising the electrolytic current, the Li content in the reduction product decreased slightly, which indicated $LiTiO_2$ was reduced as the electrolysis proceeds. $LiTiO_2$ had decomposed completely after electrolysis of 47 h. At this time, there is no Li in the product. Comparing with Li content in the porous cathode, there was no significant change in the content of CO_3^{2-} ions in melt after increasing the electrolytic current during the electrolysis. It can be deduced that CO_3^{2-} ions always were in dynamic balance in the molten salt during the subsequent electrolysis. Further, the small change in the concentration of CO_3^{2-} can also come from the addition of Li_2O in the molten salt. As a result of giving rise to CO_3^{2-}, it in turn could adversely affect the Li_2O recycling necessary for reduction of the oxide. Many studies suggest that graphite anode is also relatively less stable in low-melting LiCl-base melt than in $CaCl_2$ melt [20]. For these reasons, the graphite anode was replaced with a Pt electrode for the electrolysis.

3.4 Electrolysis with a Pt electrode

Carbon consumption and participation in electrode reactions lead to an extremely inefficient electrolysis process using a graphite electrode. Therefore, a more stable Pt anode was chosen for studying the continually-varied current electrolysis process of the porous Ti_2O_3 cathode.

Fig.8 shows the cyclic voltammograms obtained during anodic polarization of a Pt wire in LiCl-KCl-Li_2O molten salt at 800 °C.

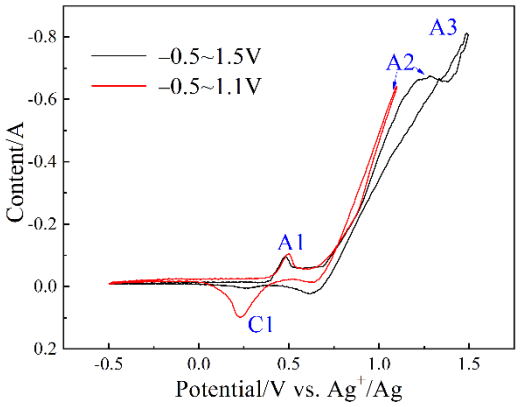

Figure 8. Cyclic voltammograms for anode polarization during different sweep range on Pt working electrode in LiCl-KCl-Li_2O melt at 800 °C.

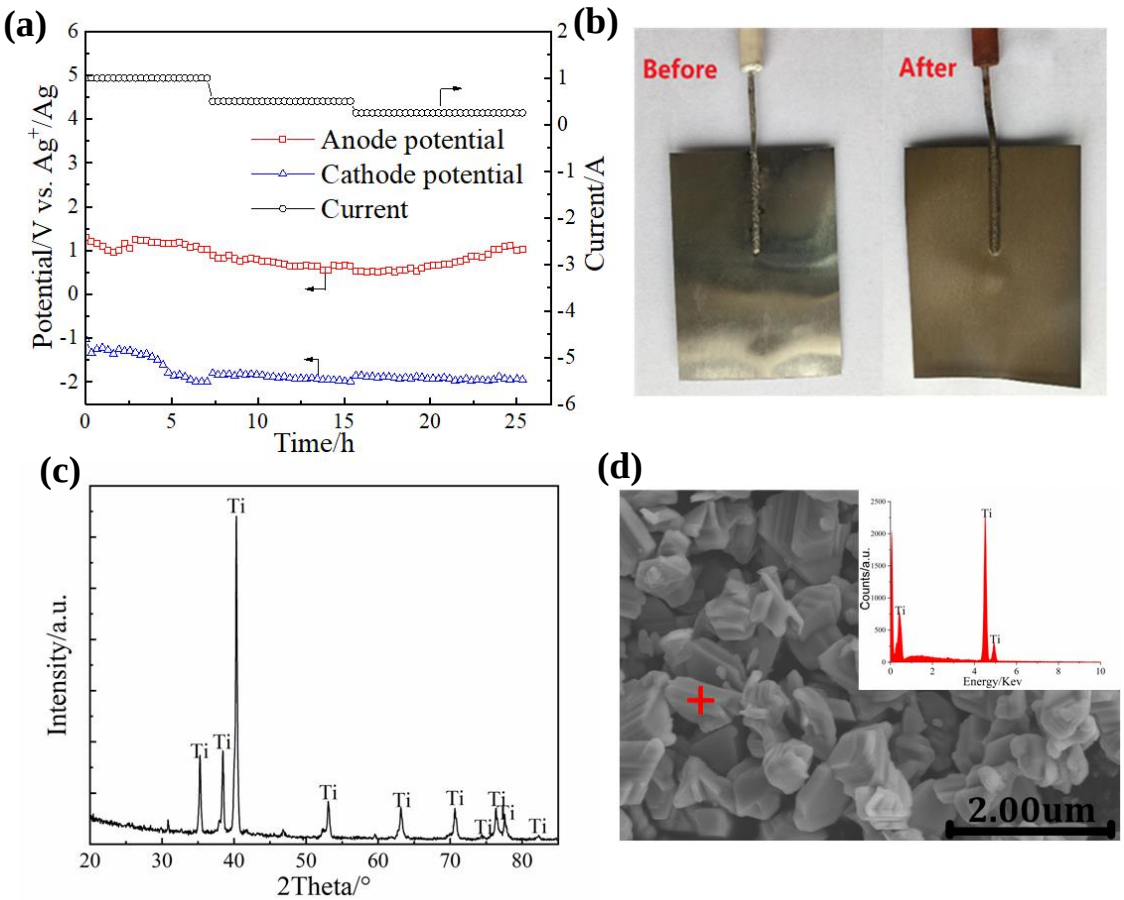

Figure 9. Electrode potentials versus time curves (a) for electrochemical reduction experiments using a Pt anode in LiCl-KCl-Li_2O melt at 800 °C; the surface appearance photos (b) of Pt anode before and after the electrolysis; the XRD spectrum (c) and SEM image (d) of the reduction product obtained after continually-varied current electrolysis for 26 h.

Three anodic wave A1, A2, and A3 and one cathodic wave C1 could be observed in Fig.8. It has been confirmed in previous studies that anodic wave A1, A2 and A3 correspond to the formation of Li_2PtO_3 coating ($2Li^+ + Pt + 3O^{2-} \rightarrow Li_2PtO_3 + 4e$), O_2 gas evolution ($O^{2-} \rightarrow 1/2O_2 + 2e$) and the dissolution of the Pt wire ($Pt \rightarrow Pt^{2+} + 2e$) respectively [21, 22]. The cathodic wave C1 corresponds to the decomposition of the Li_2PtO_3 coating ($Li_2PtO_3 + 4e \rightarrow 2Li^+ + Pt + 3O^{2-}$). Compared with the dissolution potential (1.1 V) of the Pt electrode in LiCl-KCl molten salt, that in LiCl-KCl-Li_2O molten salt shifted positively to around 1.3 V because a Li_2PtO_3 inoxidizing coating formed. However, wave C1 had weakened when the anode limit is more positive and reached 1.5 V. It indicated that the Li_2PtO_3 coating had been dissolved or exfoliated from the surface of the Pt electrode. As a result, the anode potential should be less positive than 1.3 V when a Pt sheet was used as the anode for electrolysis.

The relationships between time and electrode potentials reflect to the continually-varied current electrolysis carried out with a porous Ti_2O_3 cathode and a Pt anode in molten LiCl-KCl-Li_2O at 800 °C are presented in Fig.9a. In order to avoid the deposition of an amount of metallic Li at cathode, the cathode potential was monitored by turning down the electrolytic current gradually. When the electrolysis with 1 A for 4 h, the cathodic potential was around –1.3 V and began to have a negative shift. After electrolysis for 7 h, the cathodic potential (–2.0 V) had exceeded the deposition potential of metallic Li accompanying the electrolytic current down to 0.5 A. Accordingly, the cathodic potential shifted positively to around –1.8 V. As the electrolysis continued, the cathodic potential shifted negatively to 2.0 V after electrolysis for about 15 h again. The current was further turned down to 0.25 A.

Fig.9b shows the photos of Pt anode before and after the electrolysis. It is obviously observed that a yellow coating was formed on the surface of the Pt electrode after electrolysis, which had been identified to be Li_2PtO_3. Fig.9c shows the XRD pattern of the cathodic reduction product obtained after continually-varied current electrolysis for 26 h. The crystal structure of pure titanium was detected. The morphology of the cathodic reduction product was analyzed and shown in Fig.9d. A porous structure was found. The oxygen content of the cathode product was measured and the result showed that it was approximately 4.6%.

3.5. Discussion

Contrast with $CaCl_2$ electrolyte system, using LiCl electrolyte system has three advantages [23]: (i) The current efficiency is much better because the LiCl melt could easier permeate into the sample. Especially the porous Ti_2O_3 electrode was used in this work. (ii) Lower melting point, lower energy consumption. (iii) Avoiding the formation of refractory Ca_2TiO_3. However, only Ti-O solid solution as electrochemical reduction product can be obtained in LiCl-based molten salt. While in $CaCl_2$-based molten salt, titanium metal containing as low as 0.3% oxygen can be prepared [4, 24]. Fig.10a and b show the E-pO^{2-}diagrams of Ti-O-Cl-Li and Ti-O-Cl-Ca systems respectively [8, 25, 26]. From the diagrams, to obtain a Ti-O solid solution containing 1% oxygen as an example, it could be achieved in molten $CaCl_2$ saturated with CaO effortlessly. Whereas, a product of the same quality could be obtained with the activity of O^{2-} lower than 1.8×10^{-2} in molten LiCl requires. Thus, low-oxygen titanium was not

prepared in LiCl-based molten salt could be due to the relatively higher O^{2-} ion activity in the molten. The weaker reducibility of lithium than calcium may also be responsible for the high oxygen content of titanium products. It suggests that such an electrolytic process could be attractive for the production of Ti crude product with slightly high oxygen content [27].

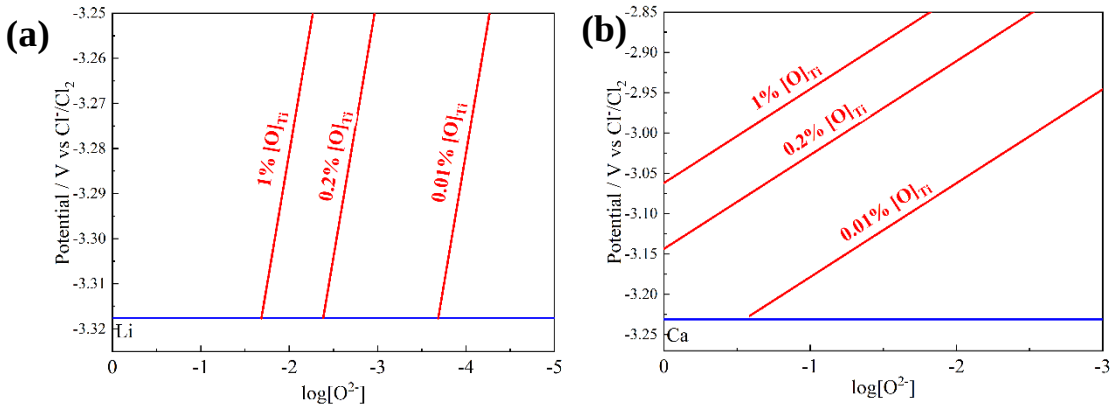

Figure 10. Diagrams of the equilibrium potential E (relative to the standard chlorine electrode) against the activity of oxide ion (expressed as its logarithm, pO^{2-}) in the systems of Ti-Cl-O-M.

5. CONCLUSION

In this work, titanium metal could be prepared via continually-varied current electrolysis of porous Ti_2O_3 electrode in molten LiCl-KCl-Li_2O at 800 °C with a graphite and a Pt anode, respectively. During the reduction process from Ti_2O_3 to Ti by electrolysis using a graphite anode, the Ti_2O_3 cathode undergoes several intermediate phases, such as $LiTiO_2$, TiO, Ti_3O, and finally metal Ti doped with TiC could be obtained. Carbonless titanium could be obtained via continually-varied current electrolysis for 26 h using a Pt anode. During electrolysis with a Pt electrode, a Li_2PtO_3 coating layer could be formed on the surface of Pt electrode at 0.5 V, which makes the dissolution potential of Pt move forward and play a protective role. In addition, the current efficiency increases greatly by the application of an inert Pt anode instead of graphite anodes. Therefore, developing a low-cost inert anode material is essential for the production of titanium by electrolysis in future. Comparing to prepare titanium in $CaCl_2$-based molten salt, the titanium product obtained in LiCl-based melt has a high oxygen content.

ACKNOWLEDGEMENTS
This research work was supported by Science and Technology Program of Chongqing, China (grant number cstc2018jcyjAX0833), and Fuling District Science and Technology Plan Project of Chongqing, China (grant number FLKJ2018BBA3075).

References

1. G.Z. Chen and D.J. Fray, *Extractive Metallurgy of Titanium*, (2020) 227.
2. C. Wu, M. Tan, G. Ye, D.J. Fray and X. Jin, *ACS Sustainable Chem. Eng.*, 7 (2019) 8340.

3. M.R. Earlam, *Extractive Metallurgy of Titanium*, (2020) 97.
4. G.Z. Chen, D.J. Fray and T.W. Farthing, *Nature*, 407 (2000) 361.
5. C. Schwandt and D.J. Fray, *Electrochim. Acta*, 51 (2005) 66.
6. K. Jiang, X. Hu, H.J. Sun, D. Wang, X. Jin, Y. Ren and G.Z. Chen, *Chem. Mater.*, 16 (2004) 4324.
7. H.S. Shin, J.M. Hur, S.M. Jeong and K.Y. Jung, *J. Ind. Eng. Chem*., 18 (2012) 438.
8. K. Dring, R. Dashwood and D. Inman, *J. Electrochem. Soc*., 152 (2005) E104.
9. D.T.L. Alexander, C. Schwandt and D.J. Fray, *Acta Mater*., 54 (2006) 2933.
10. K. Jiang, X. Hu, M. Ma, D. Wang, G. Qiu, X. Jin and G.Z. Chen, *Angew. Chem.Int. Ed.*, 45 (2006) 428.
11. C. Schwandt, G.R. Doughty and D.J. Fray, *Key Engineering Materials*, 436 (2010) 13.
12. D.S. Maha Vishnu, N. Sanil, L. Shakila, R. Sudha, K.S. Mohandas and K. Nagarajan, *Electrochim. Acta*, 159 (2015) 124.
13. R. Koc, *J. Mater. Sci*., 33 (1998) 1049.
14. A.A. Valeeva, S.Z. Nazarova and A.A. Rempel, *J. Alloys Compd*., 817 (2020) 153215.
15. Y.C. Woo, H.J. Kang and D.J. Kim, *J. Eur. Ceram. Soc*., 27 (2007) 719.
16. W. Sen, H.Y. Sun, B. Yang, B.Q. Xu, W.H. Ma, D.C. Liu and Y.N. Dai, *Int. J. Refract. Met. Hard Mater.*, 28 (2010) 628.
17. W. Sen, B.Q. Xu, B. Yang, H.Y. Sun, J.X. Song, H.L. Wan and Y.N. Dai, *Trans. Nonferrous. Met. Soc. China*, 21(2011)185.
18. J.M. Hur, J.S. Cha and E.Y. Choi, *ECS Electrochem. Lett.*, 3 (2014) E5.
19. J. Ge, S. Wang, L. Hu, J. Zhu and S. Jiao, *Carbon*, 98 (2016) 649.
20. K.S. Mohandas, *Trans. Inst. Min. Metall., Sect. C*, 122 (2013) 195.
21. S.M. Jeong, H.S. Shin, S.H. Cho, J.M. Hur and H.S. Lee, *Electrochim. Acta*, 54 (2009) 6335.
22. T.B. Joseph, N. Sanil, L. Shakila, K.S. Mohandas and K. Nagarajan, *Electrochim. Acta*, 139 (2014) 394.
23. Y. Sakamura, M. Kurata and T. Inoue, *J. Electrochem. Soc.*, 153 (2006) D31.
24. I. Park, T. Abiko and T.H. Okabe, *J. Phys. Chem. Solids*, 66 (2005) 410.
25. R. Littlewood, *J. Electrochem. Soc.*, 109 (1962) 525.
26. T.H. Okabe, R.O. Suzuki, T. Oishi and K. Ono, *Mater. Trans*., *JIM*, 32 (1991) 485.
27. K. Dring, *Key Engineering Materials*, 436 (2010) 27.